

# Preliminary Studies Of Planar Capacitance Tomography

Alan Somerville, Iwan Evans and Trevor York

Department of Electrical Engineering and Electronics, UMIST, PO Box 88, Sackville Street, Manchester, M60 1QD, UK

AS, TY and IE are members of the Virtual Centre for Industrial Process Tomography

Tel: 0161 200 4790 Fax: 0161 200 4789 email: aso@skoda.ee.umist.ac.uk

**Abstract** – Almost all previously reported applications of Electrical Capacitance Tomography (ECT) have concentrated on relatively large-scale geometries to give image resolution of the order of centimetres. There are a number of applications, for instance particle sizing, which may benefit from significantly higher spatial resolution. The present work aims, ultimately, to develop ECT for use with electrodes as small as 10  $\mu\text{m}$  wide using custom silicon technology and therefore it is natural to consider planar arrays of electrodes. This paper describes finite element simulations and measurements on laboratory scale planar arrays with the aim of identifying appropriate geometries to migrate to small scale. Preliminary results suggest that it is possible to identify bulk changes in particle size, of the order of the electrode dimensions. In addition, linear back projection has been used to produce reconstructed images of 'holes' directly above the electrodes.

**Keywords:** Capacitance, VLSI, planar electrodes, tomography.

## 1 INTRODUCTION

The work presented in this paper is aimed ultimately at the development of ECT systems using electrodes as small as 10  $\mu\text{m}$  wide. At this scale, for a 12 electrode system, the diameter of a circular sensor would be about 50  $\mu\text{m}$ . Perhaps the obvious candidate for implementing such micro-tomography sensors is integrated circuit technology which currently can offer feature sizes down to about 0.3  $\mu\text{m}$ . A significant advantage is that the processing electronics can be fabricated directly underneath the electrodes, resulting in much reduced stray capacitance. In addition, the technology offers a natural insulating layer, silicon dioxide, that can be grown over the electrodes and is also useful for protection and passivation. Previous work has explored the integration of processing circuitry for ECT [2,3]. However, the technology is inherently planar and practical realisation of circular geometries is extremely challenging. Therefore it is desirable to consider ECT systems which utilise planar arrays of electrodes that are placed along the side, rather than around, some region of interest. The use of planar arrays has been reported previously [4,5,6] to determine interface levels in three-phase separators. This paper describes preliminary investigations into planar ECT with the ultimate aim of realising capacitance micro-tomography sensors based on silicon integrated circuit technology. The

present work aims to reveal structure in the material above the electrodes. Figure 1 shows a diagram of the envisaged planar micro-capacitance sensor.

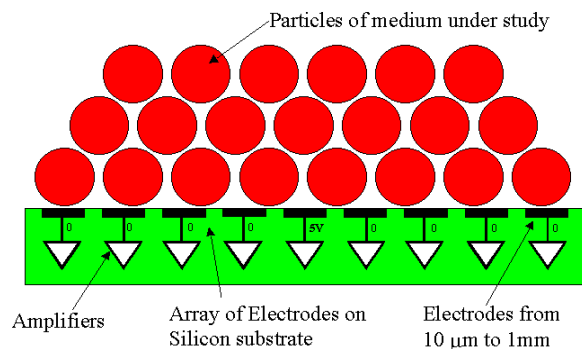


Figure 1: Planar Micro-Capacitance Sensor

The Maxwell finite element-modelling package from ANSOFT has been used to explore capacitance changes due to the introduction of materials above a planar array of sensors. To provide an indication of the effect of disturbances above planar arrays a series of simplified simulations have been performed. These consider rows of spheres placed above a pair of electrodes and the effect of electrode geometry, disturbance size, lateral and vertical displacements have been investigated. The simulations suggest sensitivity to all of these parameters and changes of

the order of 0.1 fF are predicted for the smallest arrays that have been considered up to about 0.1 pF for laboratory scale arrays.

Figure 2 and Figure 3, below, show the electric field, predicted by 3D finite element analysis, for a planar array, with and without the presence of particles above it (particles have a  $\epsilon_r$  of 16.5). It can clearly be seen from these simulations that the presence of particles, above the sensor, increases the coupling between both adjacent and non-adjacent electrodes. In Figure 2 and Figure 3 the central electrode acts as the source, with one volt applied to it, the remaining four electrodes acting as detectors.

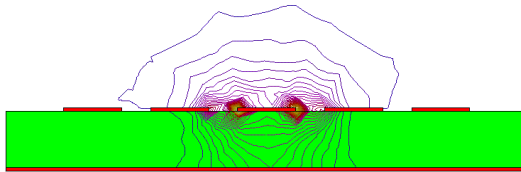


Figure 2: Sensor

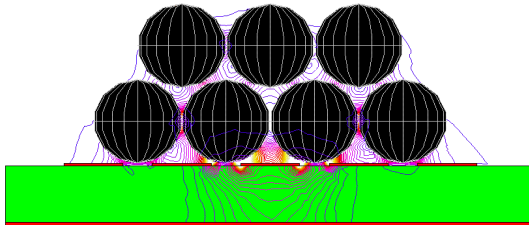


Figure 3: Sensor with particles above it

In order to deduce optimum electrode geometries a series of simulations have been conducted, and verified through experiments, on laboratory scale planar sensor arrays comprising twelve electrodes. The electrodes are 50 mm long and a variety of widths and separations have been explored. Measurements have been taken with and without layers of 'particles' above the electrodes. The use of laboratory scale experiments was necessitated by the geometric complexity of the problems being investigated. The computational requirements for finite element analysis are directly related to the geometric complexity of the problem, and with multiple objects quickly become impractical to simulate. However with experimentation the acquisition of measurement results is independent of the geometry and therefore both simple and complex problems can be evaluated quickly. The experiments explore the effect of particle size on the measurements. Two approaches have been explored for processing the measurements. Firstly an intuitive approach seeks to extract 'significant' measurements from each frame such that a metric can be deduced that classifies the layers as fine, medium or coarse grain. Secondly, a sensitivity map has been produced and from this a tomographic image is reconstructed representing a cross section through the layer.

The paper will present results from these experiments and give suggestions regarding optimum electrode geometries for planar micro-capacitance transducers suitable for implementation on silicon integrated circuits.

## 2 SIMULATION

The preliminary simulation results, generated by the Ansoft Maxwell 3D Field simulator, for linear capacitance micro-tomography have been used to determine the change in sensor capacitance, due to a disturbance placed above the sensor. It was initially intended that simulations would encompass multiple layers of spherical particles above a linear array capacitance sensor and that variations in the capacitance due to particle diameter be determined. However for relatively simple configurations, i.e. a single particle placed above the sensor, the simulation time, was found to be several hours, running on a Sun Ultra 30 workstation. Simpler geometric shapes, suitable for simpler 2D simulation, have been simulated and compared against results for multiple spheres. The uses of 2D simulation would significantly reduce the time required for simulations and thus increase the rate at which results could be obtained. Unfortunately the 2D simulations were found to give significantly greater capacitance changes than the full 3D simulations. The overly optimistic result obtained from the 2D simulations has precluded their use in providing meaningful predictions, and thus the advantages of a significantly simpler computationally task cannot be utilised. Simulations have also been performed to evaluate the use of screening electrodes, placed between the sensing electrodes, upon the sensor characteristics.

Figure 4 depicts the simplified sensor, with dimensions, used for the initial simulations. The objects to be detected are placed above and between the sensor electrodes. The sensor's electrodes and ground plane are formed from aluminium and the substrate is glass for all the simulations, with the disturbing objects (not shown), assumed to be polystyrene ( $\epsilon_r = 2.6$ ).

To allow the simulation results to be verified, simply, the simulations were scaled up to laboratory size. Disturbances due to multiple spherical objects, of various sizes, have been simulated. To simplify the simulations, the array of sensor electrodes was reduced to two, i.e. only one value of capacitance needs to be calculated. Disturbance objects of different sizes have been simulated, ranging from 5mm radius to 20mm radius. The height of the objects above the sensor was also varied between 0.5mm and 2mm.

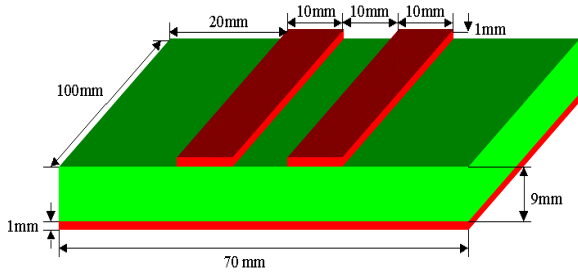


Figure 4: Simulated Sensor

## 2.1 Summary Of Results For Alternative Disturbances

The results of the 3D simulations discussed previously are summarised below in Figure 5 and Figure 6. All the simulation results presented in this paper are from 3D simulations. The changes in capacitance, caused by spherical disturbances are small. However Figure 5 clearly shows that changes in the radius of spherical disturbances produce a change in capacitance. It is very important to note, when interpreting the simulation, that as the radius of the spheres is increased fewer spheres can be placed above the sensor. The length of sensor that has been simulated is relatively short in comparison to the diameter of the larger spheres, i.e. two and a half times the largest sphere diameter. Increasing the length of the electrodes, as the particle size increases, would increase the standing capacitance of the sensor and make it difficult to compare results directly. For a micro capacitance system, where the electrodes are fabricated on the surface of a semiconductor, the ratio of electrode length to particle size could be of the same order of magnitude as these laboratory scale simulations. Figure 6 shows the change in capacitance, of the sensor, as the disturbance height is varied.

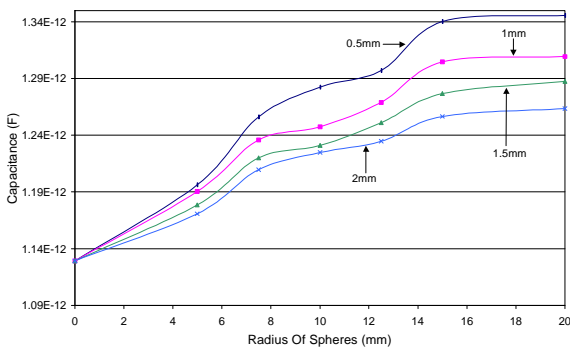


Figure 5: Total Sensor Capacitance Vs Sphere Radius at Different Heights above Sensor (Standing Capacitance shown at zero radius)

As would be expected Figure 6 show that the change in capacitance, due to the presence of a particle above the sensor, decreases in a uniform way as the height above the sensor increases. A saturation of the change in capacitance due to particle size can be

seen, from Figure 5, to occur as the particle radius exceeds one and a half times the electrode spacing.

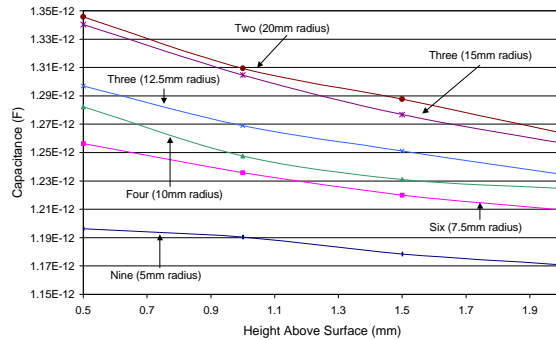


Figure 6: Total Sensor Capacitance with Height, For Multiple Spheres

## 2.2 Simulations Of Electrode Spacing on Sensor Sensitivity

To investigate the effects of electrode spacing on the sensitivity and penetration of the sensor, a series of one hundred and sixty seven 3D simulations have been performed using the simplified sensor depicted in Figure 4. The simulations have been performed for several values of electrode spacing of between one and twenty millimetres (constant electrode width of 10mm), with spheres of twenty, fifteen, ten and five millimetre radius. The spheres, of uniform size, were placed exactly midway between the sensing electrodes at a uniform height, either 0.5, 1, 1.5 or 2mm, above the sensor substrate. The number of spheres used in the simulations varied with the size of the spheres, and is summarised in table one.

Table 1: Number of Disturbing Spheres Used in Simulations

Sphere Radius	Number of Spheres
20 mm	2
15 mm	3
10 mm	4
5 mm	9

The results of these simulations are shown in Figure 7 to Figure 10 depicting the relative change in sensor capacitance (total capacitance – standing capacitance) for different disturbances as electrode spacing varies. It should be noted that due to physical constraints, simulations of particles at 0.5mm above the sensor can not be achieved for small electrode spacing (Figure 7).

It can be seen from these simulations that the smaller electrode spacing the greater the change in capacitance. However the change in capacitance due to the presence of a particle above the sensor rapidly decreases with height. A secondary interesting characteristic of these simulations, are the distinct

peaks in capacitance change with electrode spacing for different sized particles.

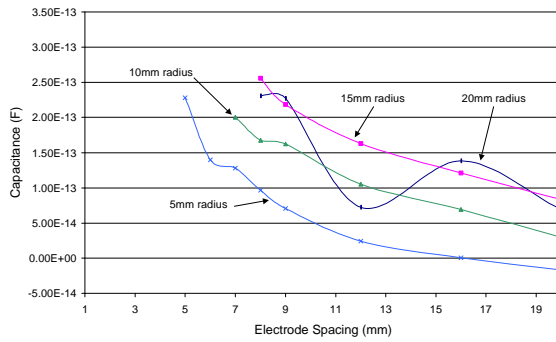


**Figure 7: Change in Capacitance Vs Electrode Spacing for Different Size Spheres at a Height of 0.5mm Above Sensor (Total Capacitance – Standing Capacitance)**

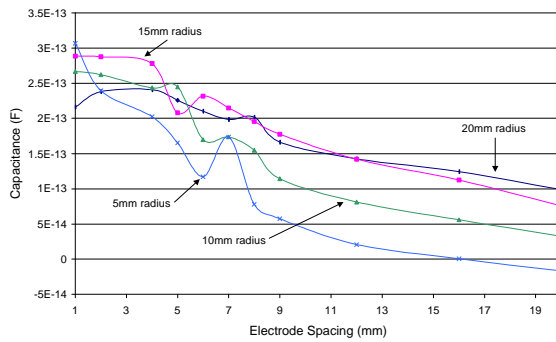


**Figure 8: Change in Capacitance Vs Electrode Spacing for Different Size Spheres at a Height of 1mm Above Sensor (Total Capacitance – Standing Capacitance)**

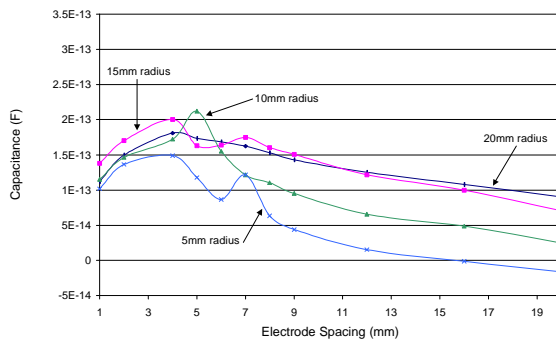


**Figure 9: Change in Capacitance Vs Electrode Spacing for Different Size Spheres at a Height of 1.5mm Above Sensor (Total Capacitance – Standing Capacitance)**

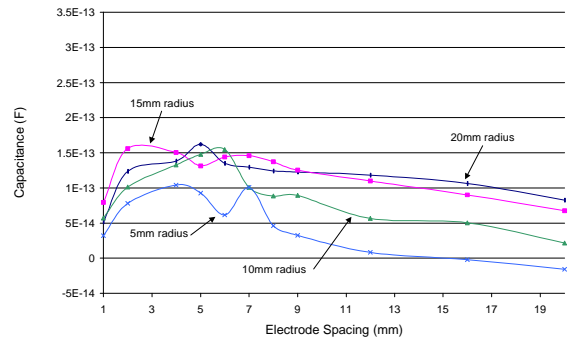


**Figure 10: Change in Capacitance Vs Electrode Spacing for Different Size Spheres at a Height of 2mm Above Sensor (Total Capacitance – Standing Capacitance)**

### 2.3 Simulations Of Sensor Sensitivity with Screening Electrodes

To investigate the effects of screening electrodes on the sensitivity and penetration of the sensor, a series of sixty-five 3D simulations have been performed using the simplified sensor depicted in Figure 11. The simulations have been performed for several values of electrode spacing of, between two and fifteen millimetres, with spheres of twenty, fifteen, ten and five millimetre radius. The spheres, of uniform size, were placed between the sensing electrodes at a uniform height, either 1, 1.5 or 2mm, above the sensor substrate (i.e. directly above central screen electrode).

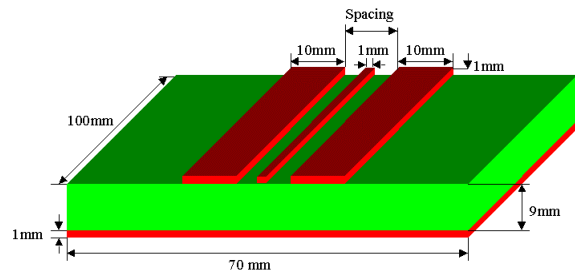


**Figure 11: Simple Sensor with Central Screen Electrode**

The results of these simulations are shown in Figure 12 to Figure 14, depicting the relative change in sensor capacitance (total capacitance – standing capacitance) for different disturbances as electrode spacing varies. It can also be seen from these simulations that the addition of screening electrodes has caused little change in sensor sensitivity. However the screened electrodes have virtually eliminated the peaks in the capacitance change, providing much more predictable behaviour.

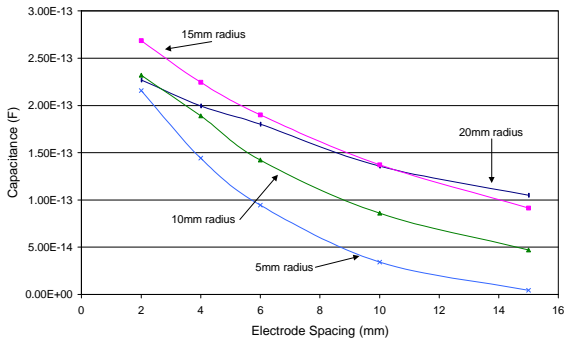


**Figure 12: Change in Capacitance Vs Electrode Spacing for Different Size Spheres at a Height of 1mm Above Sensor with Screen Electrode (Total Capacitance – Standing Capacitance)**

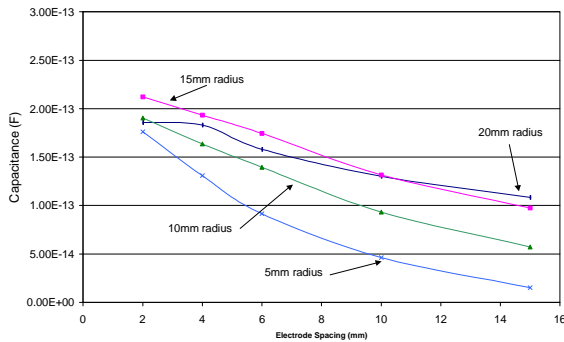


**Figure 13: Change in Capacitance Vs Electrode Spacing for Different Size Spheres at a Height of 1.5mm Above Sensor with Screen Electrode (Total Capacitance – Standing Capacitance)**

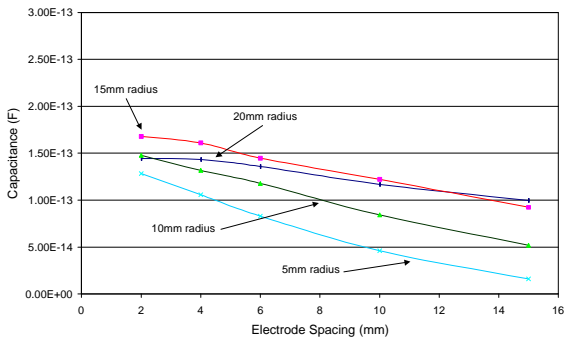


**Figure 14: Change in Capacitance Vs Electrode Spacing for Different Size Spheres at a Height of 2mm Above Sensor with Screen Electrode (Total Capacitance – Standing Capacitance)**

## 2.4 Discussion of Simulation Results

The relatively poor sensitivity of the sensor to spherical disturbances may be improved by increasing the electrode length, to allow a greater number of spheres to sit above it. This increase in length would also have the effect of increasing the sensors standing capacitance. The results show that the total capacitance, both standing and disturbance, of the sensor drops rapidly as the electrode spacing is

increased. However it can also be seen from these graphs, that the presence of disturbances (i.e. the spheres above the sensor) does cause a change in the capacitance of the sensor. The change in sensor capacitance, due to disturbances, can be seen clearly in Figure 7 to Figure 10. Interestingly these results show peaks and troughs in the size of capacitance change against electrode spacing curves, for different sized disturbances. These peaks and troughs could potentially provide very useful tomographical information from sensors with multiple electrodes of different spacing. However, further experimental work must be undertaken to determine whether this peaking effect is real or simply a simulation error. The addition of screening electrodes to the sensor reduces the standing capacitance of the sensor. It can also be seen from Figure 12 to Figure 14, that the addition of screening electrodes has not caused much change in maximum sensor sensitivity to disturbances. However the screened electrodes have virtually eliminated the peaks and troughs in the capacitance change against electrode spacing curves, providing, apparently, much more predictable behaviour.

These results indicate that tomographical information can be obtained from a linear array sensor. However laboratory experiments will have to be performed to confirm these results, and extend them to include multiple electrodes in the presence of many layers of disturbance particles. The peaking of sensor sensitivity, without screen electrodes, for different size disturbances at different electrode spacing indicates that a graduated spacing of multiple electrodes may be highly beneficial.

## 3 LABORATORY SCALE SENSORS

To confirm the simulation results, presented in the previous section, and extend the investigation, a set of laboratory scale sensor arrays has been fabricated. The sensor arrays have been manufactured on PCB and consist of twelve electrodes, 50mm in length, above a ground plane. Electrode widths of 5mm and 2mm have been implemented, with spacing of 5mm and 2mm. Sensor arrays with grounded electrodes of 4mm or 1mm width between the sensing electrodes have also been implemented.

To simulate the presence of particles above the sensor array, two sizes of glass marbles ( $\epsilon_r = 5.5$ ), 15mm and 25mm diameter, have been employed. Multiple layers of the marbles being randomly placed on the sensor array. To determine the dynamic range of the sensors, coupling capacitance was measured with nothing above the sensor (empty) and seven sheets of 5mm thick Glass (full).

The measurement of capacitance, between the electrodes of the laboratory scale sensors, was achieved using a HP4192A Impedance Analyser, connected via a multiplexing box to the sensor array. The changes in capacitance for these laboratory scale sensors, due to the presence of marbles above them, is

very small and near the lower limits of the Impedance Analyser. To reduce the effect of the limited resolution of the Impedance Analyser, multiple readings were taken.

### 3.1 Results From Laboratory Scale Sensors

A selection of the results obtained from the laboratory scale sensors are shown in Figure 15 to Figure 18 and are typical of the results obtained for all the sensors. The presented results depict the change in the sixty-six independent capacitance readings, due to a disturbance, for a twelve-electrode sensor.

The sixty-six capacitance readings are depicted in Figure 15 to Figure 18 as a continuous plot. The first eleven values of the results, depict the capacitance values when electrode one is the source (i.e. the first value is the capacitance between electrode one and two and the eleventh reading is the capacitance between electrode one and electrode twelve). The twelfth value depicts the capacitance between electrode two and electrode three, when electrode two is acting as the source, etc.

It can clearly be seen from Figure 15 to Figure 18 that a metric exists, which makes it possible to distinguish between large and small marbles above the sensor. It can also be seen from Figure 16 to Figure 18 that it is possible to distinguish between a mixture of large and small marbles and layers of single size marbles. Unfortunately the results from the laboratory scale sensors, are inconclusive in terms of indicating the optimum sensor configuration and geometry. This disappointing result is probably due to the limited resolution of the Impedance Analyser used for these experiments. However close study of Figure 18 (the sensor with varied spacing between the electrodes) indicates that the change in capacitance between electrodes is sensitive to both the particle size and electrode spacing i.e. the metric between large, small and mixed layers of marbles changes over the length of the sensor.

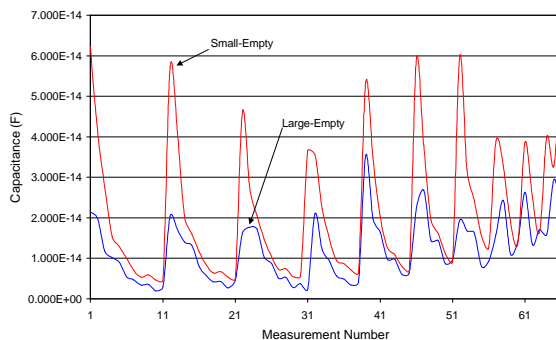


**Figure 15: Average Change In Capacitance Due to Layer of Glass Marbles (12 Electrodes 50mm Long, 5mm Wide with 5mm Spacing)**

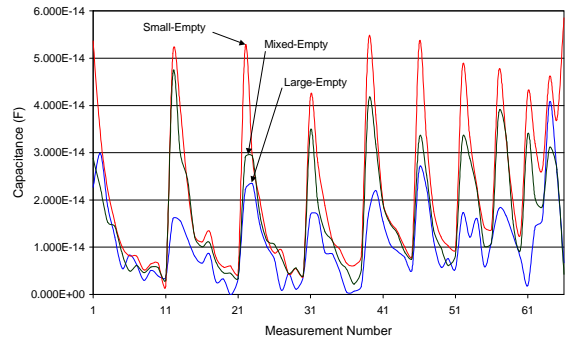


**Figure 16: Average Change In Capacitance Due to Layer of Glass Marbles (12 Electrodes 50mm long, 5mm wide, 5mm Spacing with 1mm Grounded Electrodes Between Them)**

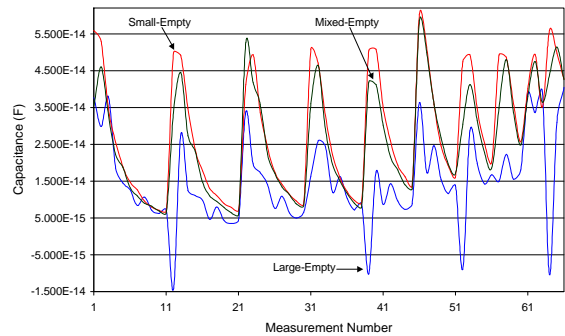


**Figure 17: Average Change In Capacitance Due to Layer of Glass Marbles (12 Electrodes 50mm Long, 5mm Wide with 2mm Spacing)**

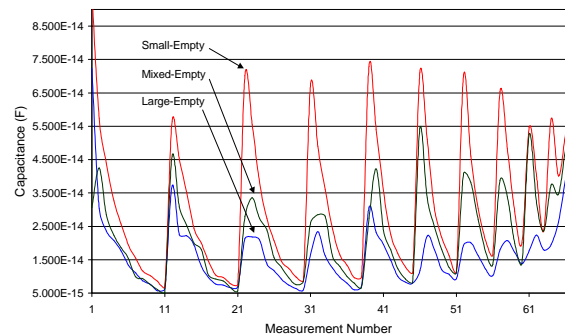


**Figure 18: Average Change In Capacitance Due to Layer of Glass Marbles (12 Electrodes 50mm Long, 5mm Wide with Spacing Varying Linearly From 1mm to 5mm)**

### 3.2 Image reconstruction

Using the first sensor (Figure 15) image reconstruction has been achieved using back-projection [7]. A sensitivity map was generated from actual measurements made using, precision cut, blocks of Tufnol ( $\epsilon_r \approx 5$ ), arranged in four layers above the sensor. Each layer of Tufnol was 12mm thick. Using equation 1, the sensitivity of each location, physically defined by the gaps in the Tufnol blocks, was calculated from actual measurement results.

$$(1) \quad S_{i,j}^{(k)} = \left( \frac{1}{b^{(k)}} \right) \frac{C_{i,j}^{(k)} - C_{i,j}^{(full)}}{C_{i,j}^{(empty)} - C_{i,j}^{(full)}} \quad (k=1, \dots, K)$$

Where  $C_{i,j}^{(k)}$  is the capacitance when the  $k^{\text{th}}$  position above the sensor is empty.  $C_{i,j}^{(empty)}$  and  $C_{i,j}^{(full)}$  are, respectively, the capacitance when the sensor has nothing above it and four layers of Tufnol.  $b^{(k)}$  is the fractional area of the  $k^{\text{th}}$  element above the sensor.

Using this sensitivity map the images shown in Figure 19 and Figure 20 have been reconstructed, and clearly show holes in the first Tufnol layer, above electrode one and six, respectively.

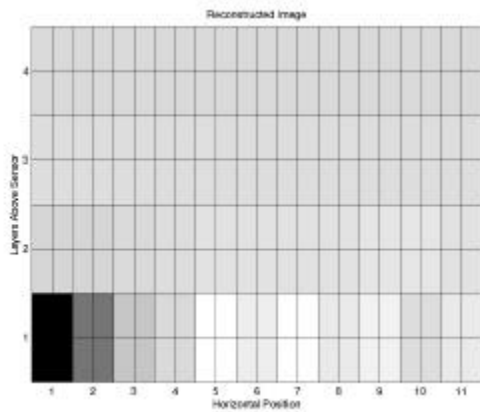


Figure 19: Reconstructed Image of Hole above Electrode One

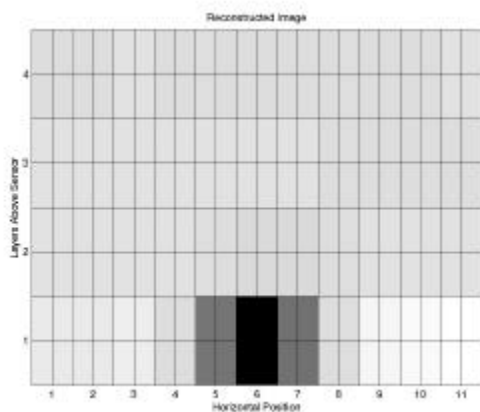


Figure 20: Reconstructed Image of Hole above Electrode Six

In Figure 19 and 20 the darker region representing the absence of material above the sensor, and conversely the lighter regions the presence of material. However, image reconstruction of features within the second, third and fourth layers of Tufnol failed to produce discernible images of the feature. Several factors can be attributed to this failure, such as

the limited resolution of the impedance analyser, the relatively thick layers of Tufnol used, the use of multiple layers forming a laminar structure and the relatively inaccuracy of the image reconstruction technique [8].

#### 4 CONCLUSIONS

The results presented in this paper, both simulated and measured, show that planar arrays can give qualitative information about materials placed above them. Both simulation and experimental results, however, also indicate that graded electrode spacing could provide better qualitative information than a uniform array.

It is also clear from these results, that electrodes with dimensions as small as 10µm will require capacitance measurement to a very high precision, in the order of sub femto farads. The requirement for very high precision capacitance measurement can clearly be seen from the failure of the laboratory scale experiments to provide sufficient resolution to enable image reconstruction of features not directly above the sensor surface. The simplicity of the image reconstruction technique employed, and its consequential relative inaccuracy, also compounds the need for very precise capacitance readings. The use of a more sophisticated image reconstruction algorithm, combined with a more accurate impedance analyser and thinner layers of dielectric, should allow image reconstruction of features that are not in direct contact with the sensor surface.

The change in capacitance of a planar array, due to a disturbance above it, decreases rapidly with the height of the disturbance. The height above the sensor at which changes, or features, in the material placed on the sensor can be detected is hard to determine. The technique and implementation of the capacitance measurement, and consequent resolution, will clearly have a very large influence on the final depth sensitivity. Many other factors will influence the depth penetration of a planar array sensor, such as the electrode size, electrode spacing and the material placed under study. However it is hoped that disturbances at heights of approximately 10% of the sensor length (or width assuming a square total sensor area) will be measurable.

## REFERENCES

- [1] Williams R.A., Gregory P.J., Luke S.P., Dickin F.J., Gate L. and Taylor S.P., '*Microelectrical Resistance Imaging of Flowing Colloidal Dispersions*', Proc. Frontiers in Industrial Process Tomography, San Luis Obispo, California, USA, October 1995, 335.
- [2] Chan P.K., Bozic M. and York T.A., '*Custom Integrated Circuits for Tomographic Imaging Systems*', Proceedings of the European Concerted Action on Process Tomography, Oporto, Portugal, March 24th-26th, 1994, 123-134.
- [3] Haycock R.J., Williams P.M. and York T.A., '*Integrated Electrodes for Electrical Capacitance Tomography*', IEEE Instrumentation and Measurement Technology Conference, St. Paul, Minnesota, USA, May 19-21, 1998, 472-475, (ISBN 0-7803-4797-8).
- [4] Yang W.Q, Brant M.R. and Beck M.S., '*A Multi-Interface Level Measurement System Using a Segmented Capacitance Sensor for Oil Separators*', Meas.Sci.Tech., 5, 1994, 1171-80.
- [5] Wang H, Yin W, Yang W.Q. and Beck M.S., '*Optimum Design of Segmented Capacitance Sensing Array for Multi-Phase Interface Measurement*', Meas.Sci.Tech., 7, 1996, 79-86.
- [6] Wang H and Yin W., '*A Study of the Detection Mechanism and the Reconstruction Algorithm for Multi-Phase Interface Level Measurement*', Meas.Sci.Tech., 8, 1997, 1289-1294.
- [7] R. A. Williams and M. S. Beck '*Process Tomography – Principles, Techniques and Applications*' Butterworth Heinemann Ltd, Oxford, 1995.
- [8] M. Wang, R. Mann and F.J. Dickin '*Electrical Resistance Tomographic Sensing Systems For Industrial Applications*', Chem. Eng. Comm, 1998, Vol. 00, pp. 1-22.